Evaluation Study on Wavelet Denoising of Antenna-Based PD Measurements in Strong Interference Environments Considering a New Reliability Score of Pulse Detection

Kerstin Friebe and Frank Jenau

***Abstract*— Partial discharge (PD) interference suppression represents an important aspect in the diagnosis and maintenance of equipment in the power transmission network and thus contributes to ensuring transmission reliability. PD diagnosis includes the detection of PD using suitable measurement methods like non-contact electromagnetic methods such as antennas. An important step of measuring PD with antennas is the interference suppression of the measurement signals for further processing. Especially in the case of contactless detection of PD using antenna structures, other signals are coupled in addition to the actual PD signal. This requires interference suppression processes for pulse extraction of the PD pulses from the disturbed signal as well as evaluation criteria that measure the interference suppression and the reliability of the PD pulse detection of these processes. In the context of this work, a suitability study is carried out to select the mother wavelets and estimation methods within the framework of wavelet denoising. This is done by a preliminary study with synthetic signals in which a real noise environment is added, which is several times stronger than the synthetic PD signal. The best combinations are then applied to real PD signals measured in a strong interference environment. In addition to the conventional evaluation criteria for noise reduction and signal distortion, a new evaluation criterion, the reliability score of impulse detection, is introduced. The methodical approach also reliably determines whether generated PD are isolated, as a transmission line-bound reflection-free decoupling of the PD signal takes place simultaneously.**

***Index Terms*— HVDC, interference suppression, partial discharge (PD), pulse detection, wavelet denoising.**

I. Introduction

A. Motivation-Interference During PD Measurements

THE interferences during partial discharge (PD) measurements vary depending on the environmental and measurement conditions. External sources of interference that require consideration with regard to PD measurements according to IEC 60270 are listed in [1]. Possible sources of interference in a more general context are described in [2]. In [1], differentiation is made between interference that occurs even when the test setup is not in operating mode and interference that only occurs during the operation of the test setup. This classification refers to measurement methods for the explicit testing of PD. For this purpose, at least one voltage source for loading the device under test and further measuring components are required for the PD test and represents a source of interference itself.

Interferences that predominate independently of the test operation are powerful narrowband interferers such as broadcast transmitters, e.g., mobile radio and WIFI communication channels. Broadband disturbances such as switching operations and commutation machines in dc voltage sources in the immediate environment or the inherent noise of the measuring instrument itself also represent disturbances that are superimposed on the PD signal [1], [2].

Contactless acquisition by a broadband antenna prevents interference caused by the test circuit itself and does not accumulate interference that is already present. Since the components are tested in operation or are loaded with a test voltage, these test operations-related disturbances defined in [1] still occur as environmental disturbances. In addition to the disturbances already mentioned, there are disturbances in the form of PD in components that are part of the test or in the test environment, as well as contact noise and sparks at poorly designed connections and bushings. Not negligible are harmonics on the power supply side that are transmitted into the system [1], [2].

B. State-of-the-Art Interference Suppression by Digital Signal Processing

Beside digital filters such as recursive filters (IIR filters), nonrecursive filters (FIR filters), and the Wiener filter, which are used to suppress narrowband periodic interferers [3], [4], the wavelet denoising method based on the discrete wavelet transform (DWT) offers an alternative that also reliably suppresses broadband interferers and noise. Wavelet denoising introduces several application-dependent combinations of the following parameters [5], [6], [7]:

Manuscript received 6 November 2023; revised 9 January 2024; accepted 1 March 2024. Date of publication 7 March 2024; date of current version 19 December 2024. This work was supported by the TU Dortmund University. *(Corresponding author: Kerstin Friebe.)*

The authors are with the Institute of High Voltage Engineering, TU Dortmund University, 44227 Dortmund, Germany (e-mail: kerstin.friebe@tu-dortmund.de).

Digital Object Identifier 10.1109/TDEI.2024.3374243

1) wavelet family and wavelet of family;
2) number of levels of decomposition;
3) threshold rule;
4) method of estimate threshold value;
5) method for estimating the variance of the noise.

Several studies on the wavelet selection are available. The Daubechies Wavelet (db), designed around 1990 by Ingrid Daubechies, as well as the Coiflet Wavelet (coif), also designed by her, and a modified form of the Daubechies Wavelet, the Symmlet Wavelet (sym), are already subject of research on interference suppression of PD measurement signals [8], [9], [10], [11], [12]. These wavelet families mentioned are orthogonal wavelets. Biorthogonal wavelets such as the BiorSplines Wavelet (bior) are also suitable for interferer reduction of PD measurement data [10].

There are also approaches to energy-based selection of wavelets [13] and correlation-based selection of wavelets [14] in the context of interference suppression of PD measurement signals.

In addition to the choice of wavelet, the interference suppression performance of wavelet denoising is also affected by the choice of threshold rule. Several combinations of the hard and soft threshold rule with chosen wavelets are performed in [8], [10], [12] and [15]. In [15], the threshold function is adjusted to adapt the threshold value to the noise level of the environment. In [16], a new threshold function is developed that combines the advantages of the hard and soft threshold rule. An energy-based approach to the threshold rule is investigated in [17].

Moreover, the wavelet interference suppression method is compatible with other filters and in combination with itself by varying parameters [18]. Besides methods for interference suppression of PD measurements using the DWT, there are comparable methods for interference suppression of PD measurement signals with the variational mode decomposition and the multiscale principal component analysis [19].

The investigations differ in the choice of the sensor for measuring the PD, which results in differences in the possible interference coupling. This is associated with differences in the interference level and, correspondingly, the signal-to-noise ratio (SNR) of the data to which wavelet denoising is applied. Conventional measuring circuits with coupling capacitor and measuring impedance are used in [9], [10] and [13] to decouple the PD signal. This results in PD signals with an SNR of 69 dB [10] and −16 dB [13]. Within [11] and [12], an RC detector is used on the grounding cable, resulting in an SNR of 13.7–37 dB.

The PD signal is detected inductively in [17] using a Rogowski coil and an acoustic sensor on an oil tank with a PD source and RF antenna inside the tank. The PD signals have an SNR of up to −5 dB.

A UHF antenna inside an oil tank with the PD source is used in [14]. This results in an SNR of 1–5. A monopole antenna of 5 cm length is used outside the test object in [19]. The PD signals have an SNR of up to −10 dB. A piezoelectric ultrasonic sensor is mounted in an oil tank in [15], in which a needle-plate arrangement is located. The PD signals have an SNR of 6.16 dB.

The accumulation of free metal particles on the surface of the gas-insulated switchgear internal insulation structure is imitated in [16] and measured with an acoustic emission sensor mounted on the outside. This results in PD signals with an SNR of up to −20 dB.

The location of faults in a power cable in [20] is carried out with just one sensor instead of two as usual. Wavelet denoising is used here to improve the accuracy of the location. The PD signals have an SNR of −15 dB.

Synthetic PD signals are superimposed in [18] with a noise level of 50%, which corresponds to an SNR of 0.16. Synthetic signals with an SNR of 30–40 dB are used in [8].

Common to all studies is the use of quantitative evaluation criteria. For evaluation of interference suppression processes, besides the already mentioned SNR, parameters such as the noise reduction level (RNL) [9], [17] or noise reduction ratio (NRR) [15], [19] are commonly used. Parameters such as the root mean square error (RMSE) [15], [17], [18] or mean square error (MSE) [10] and the correlation coefficient (Corr) [8], [15], [19] are used to evaluate the influence of the interference suppression process on the input useful signal.

C. Contribution and Outline

In this work, a classical logarithmic periodic antenna is used to detect the PD signal. Non-contact detection by broadband antennas allows the detection of PD during operation without requiring intervention in the equipment or surrounding infrastructure. A broadband detection increases the information content of the detected PD signal, which improves the subsequent feature identification of different PD types. The PDs are generated with a needle-plane arrangement. The measurement is carried out in a high-voltage laboratory, which has a strong interference environment. This is caused by-in addition to the influences mentioned in [1] and [2] high voltage and high frequency laboratories in the nearer environment as well as reflections on the high voltage cage. This represents a strong interference environment as expected in other high voltage laboratories and converter halls. Due to the broadband nature of the antenna, these interferences couple into the measurement signal over a wide frequency range. The PD signals obtained this way have an SNR of about −60 dB. Due to this, the PD signals are not detectable in the measured signal without interference suppression.

The suitability of wavelet denoising for the suppression of PD signals, which are detected with broadband logarithmic periodic antennas in a strong interference environment, is demonstrated by an evaluation study with synthetic and real measured PD signals. The study examines extensive combinations of wavelets, threshold rules, and threshold estimation methods in order to determine the best combination for denoising PD signals detected with broadband antennas. The possibility of time synchronous measurement of a reflection-free comparison signal also allows the evaluation of the pulses contained in the interference suppressed signal as true PD pulses or interference pulses that are not filtered out. This introduces a new evaluation criterion, the reliability score of pulse detection.

The structural process in the work is as follows.

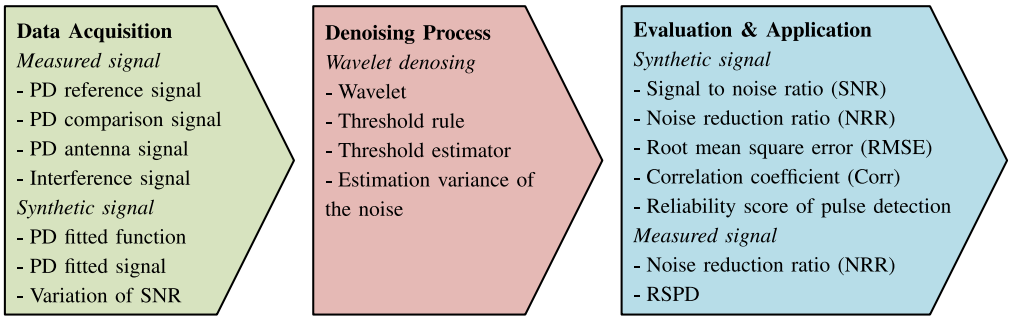

Fig. 1. Methodical approach of the studies.

TABLE I
OVERVIEW OF THE REALIZED INVESTIGATIONS WITH WAVELET FAMILIES, SELECTED WAVELETS FROM THE FAMILIES, THRESHOLD ESTIMATION, AND THRESHOLD RULE

Wavelet		Threshold estimation & rule
Wavelet family	**Selected wavelets**	
Orthogonal wavelets		
• Best-localized Daubechies	• bl7, bl9, bl10	• Universal hard
• Beylkin	• beyl	• Universal soft
• Coiflets	• coif1, coif3, coif5	• Bayes hard
• Daubechies	• db4, db10, db25	• Bayes soft
• Fejér-Korovkin Filter	• fk8, fk14, fk22	• Minmax hard
• Han linear-phase moments	• han3.3, han4.5, han5.5	• Minmax soft
• Morris mini.-bandwidth	• mb10.3, mb14.3, mb32.2	• FDR hard
• Symlets	• sym4, sym10, sym25	• SURE hard
• Vaidyanathan	• vaid	• SURE soft
• Discrete Meyer	• dmey	
Biorthogonal wavelets		
• BiorSplines	• bior1.5, bior3.9, bior6.8	
• ReverseBior	• rbio3.9, rbio5.5, rbio6.8	

1) data acquisition with logarithmic periodic antenna and of time synchronous reflections-free comparison signal in strong interference environment;
2) simulation of a synthetic signal with a strong interference level;
3) study on wavelet, threshold estimator, and threshold rule with synthetic signal;
4) evaluation of signal distortion, interference suppression, running time, and reliability of pulse detection;
5) application of the best-identified combinations of wavelet, threshold estimator, and threshold rule to measurement data;
6) evaluation of interference suppression of the measurement data, running time, and reliability of pulse detection.

II. METHODICAL APPROACH

In Fig. 1 the process of the evaluation of the wavelet denoising in the context of the PD diagnosis is shown. It consists mainly of data acquisition, the actual denoising process, and the following evaluation and application.

The data acquisition is divided into the generation of measurement data and the generation of the synthetic signal. The measurement setup shown in Fig. 2 is used to generate the measurement data. The special characteristic of this measurement setup is, that the PDs are generated within a measurement cell which, due to its impedance of 50 Ω, enables an interference-free decoupling of the PD signal via a coaxial cable. The signal is recorded synchronously with the antenna signal and thus enables the successful detection of the PD signals in the measurement signal of the antenna to be evaluated. The antenna is a classical logarithmic periodic antenna. To detect and represent the real interference environment, the antenna is also used to record an interference signal with the source turned on at an output voltage of 0 V. For measuring the PD reference signal, a copper wire as shown in Fig. 2 is used to detect an electromagnetic PD signal, which is assumed to be largely unaffected by interference.

The synthetic signal enables an evaluation of the interference reduction and the influence of the interference suppression process on the input signal. Hereby, the output signal of the interference suppression process is compared with a known input signal and both—the interference suppression and the distortion—are evaluated with criteria. Real measurement data are not suitable for this purpose, since the real PD signal is superimposed with interference in the measurement signal and is therefore unknown. By this fact, the actual interference suppression process is motivated. To generate the synthetic signal, the PD signal measured using the reference wire signal is fit with a mathematical function and synthesized in continuous sequences to the synthetic PD signal. The interference signal measured under real laboratory conditions is added to this synthetic PD signal. To realize

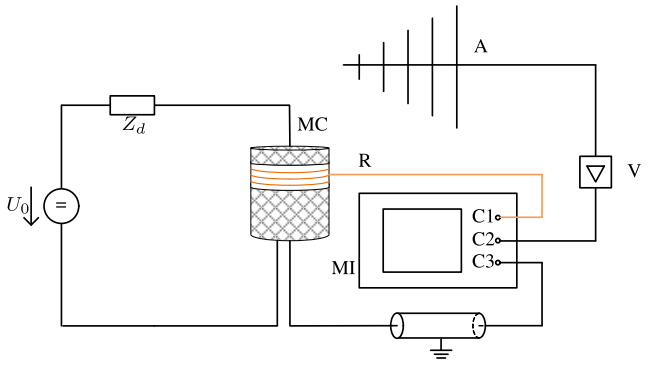

Fig. 2. Measurement setup with antenna (A), amplifier (V), reference wire (R), MC, MI, decoupling impedance Z_d, test voltage U_0.

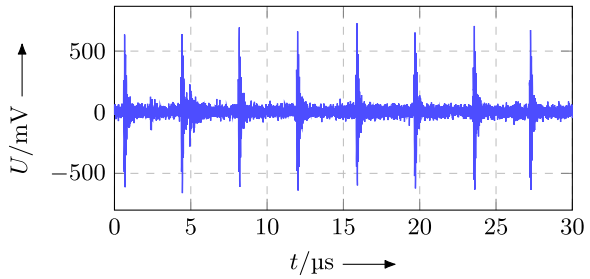

Fig. 3. PD reference signal (R)-section of a signal with over 100 PD.

a variation of the SNR, the synthetic PD signal is scaled varying.

The interference suppression process is realized by the wavelet denoising. There are different possibilities of variation from the selection of the wavelet family, over the threshold estimation up to the threshold rule. In the de-interference process, the synthetic PD signals are fed to the wavelet denoising by varying the parameters shown in Table I. All listed wavelets as well as estimation methods and threshold rules are tested and the most suitable combinations based on the evaluation criteria are presented.

The evaluation is carried out with criteria, which on the one hand evaluate the noise suppression and the PD impulse detection and on the other hand with criteria, which evaluate the influence of the interference suppression process on the PD signal. The SNR before and after the interference suppression and the NRR are used to evaluate the achieved interference reduction. The reliability score of pulse detection RSPD indicates how many of the PD pulses are detected in the signal by the interference suppression process. The RSME and Corr between the input signal and the output signal are used to quantify how much the interference suppression process affects the input signal. This includes interference components that are not filtered out by the interference suppression process. To check the suitability of the method for use in online monitoring, the running time Δt is determined.

The best combinations resulting from the study with synthetic PD signals are applied to the measured PD signal. Finally, the SNR is estimated and the NRR after interference suppression is calculated. The reliability score of pulse detection RSPD and running time Δt are also determined.

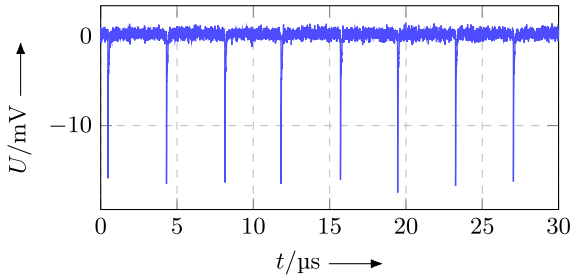

Fig. 4. PD comparison signal (MC)-section of a signal with over 100 PD.

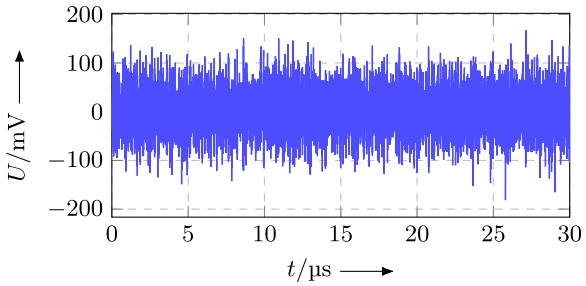

Fig. 5. PD antenna signal (A)-section of a signal with over 100 PD.

III. Data Acquisition

A. Measurement Recording of PD Signals

The measurement is performed using the measurement setup shown in Fig. 2. In the measuring cell (MC) a needle-plane arrangement is located, to which dc high voltage U_0 is applied to generate PD pulses. A copper wire (R) is placed around a plastic ring of the measurement cell to detect the electromagnetic PD reference signal, which is shown in Fig. 3. Due to its conical design, the measurement cell has a characteristic impedance of 50 Ω, allowing reflection- and interference-free measurement of the PD current. Using a coaxial cable on the ground side, the signal from the cell is transferred to the oscilloscope measurement instrument (MI). Since this signal, shown in Fig. 4 is interference-free and is clearly assigned to the PD pulses, it is used as a comparison signal for later evaluation of the reliability score of pulse detection. Thus, it is used as a comparison to indicate using a reliability score of pulse detection RSPD how many of the PD pulses are actually contained in the interference-suppressed signal or are incorrectly eliminated from the signal. In addition, the remaining interference pulses are identified as such.

The non-contact detection is performed by a log-periodic antenna (A) with a bandwidth of 30–2000 MHz, whose measurement signal is forwarded to the oscilloscope MI via an amplifier (V) with linear gain by a factor of 100 in the range of the antenna bandwidth. The oscilloscope has an analog bandwidth of 4 GHz and is used with a sampling frequency of 20 GHz. The measurement signals are recorded time-synchronously on all channels. This enables the mentioned evaluation of the successful detection of PD pulses and the identification of remaining interference pulses by using the comparison signal. The contactless acquired signal is shown in Fig. 5. Clearly, visible is the superposition of the PD pulses with interference, which makes detection and subsequent analysis of the PD pulses impossible without data processing. An interference signal is also detected by the

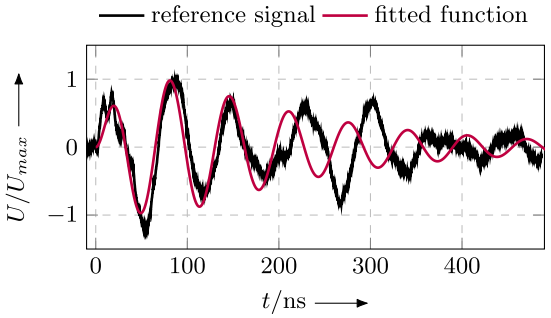

Fig. 6. Synthetic PD pulse fit to reference signal.

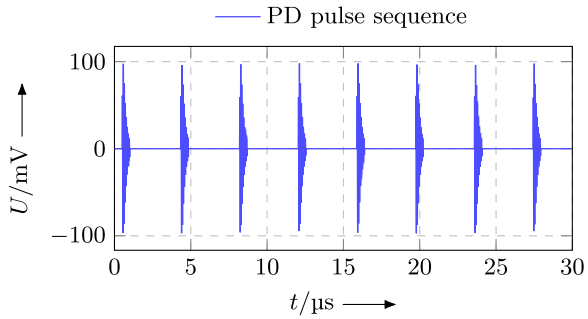

Fig. 7. Synthetic PD pulse sequence-section of a signal with over 100 PD.

antenna while the source is switched on and a voltage of 0 V is applied.

B. Synthetic PD Signals

The synthetic PD signal is generated by a product of a rising exponential function, a falling exponential function, and an oscillating function defined by

$$f(t) = A_1 e^{-t/\tau_1} \cdot A_2(1 - e^{-t/\tau_2}) \cdot \sin(2\pi f_0 \cdot t). \tag{1}$$

The PD reference signal detected by the copper wire is used as the target signal in this case. To fit the mathematical function to this PD signal, 100 PD reference pulses are recorded with the comparison signal as a trigger using a sequence measurement mode. These pulses are first averaged and then the variables in (1) are iteratively adjusted. Both signals are plotted in Fig. 6. To produce a time signal containing over 100 PD pulses, the fit function is continuously repeated, taking into account the repetition rate in the PD reference signal. A section of the PD signal synthesized in this way is shown in Fig. 7.

The synthetic PD signal and the interference signal measured with the antenna under real laboratory conditions are superimposed to generate an interfered PD signal. Here, the addition of the samples to a new total amplitude is performed as shown in Fig. 8. To model signals with different SNRs, the amplitude A of the synthetic PD signal is varied before adding to produce a corresponding SNR. An amplitude of $A = 0.1$ V corresponds with an SNR of -24.5 dB, an amplitude of $A = 0.03$ V corresponds with an SNR of -48.57 dB and an amplitude of $A = 0.01$ V corresponds with an SNR of -70.55 dB. Signals with a large negative SNR are especially representative of broadband and contactless detected PD signals, as they contain a lower energy level than ambient noise and interferers, which are also detected by broadband contactless antennas.

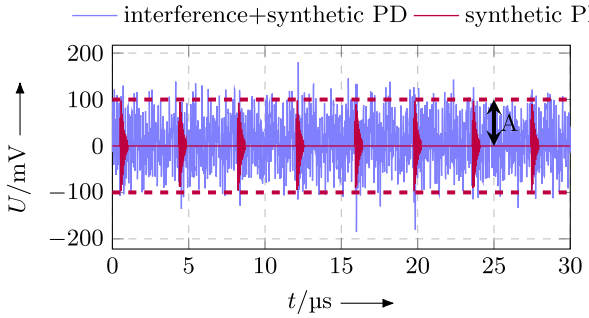

Fig. 8. Synthetic PD signal superimposed with interference (SNR = $-$**24**, **5** dB and A = **0**, **1** V)-section of a signal with over 100 PD.

IV. Denoising Process

In the context of wavelet denoising, after the DWT a manipulation of the wavelet coefficients is performed according to certain decision rules. After this, the signal is subsequently transformed back by an inverse DWT (see Fig. 9).

A. Wavelet Transformation

The base function

$$\psi_{\varsigma,\tau}(t) = \frac{1}{\sqrt{\varsigma}}\,\psi\left(\frac{t-\tau}{\varsigma}\right) \tag{2}$$

is called base wavelet or mother wavelet [5], [21]. By varying the scale factor ς and translational τ, the wavelet is compressed or stretched and shifted along the analyzed signal. The compression and stretching affect the center frequency and bandwidth of the resulting bandpass filter [5]. In analogy to the frequency in the context of the FFT, during a WT so-called scales are used, which are inversely proportional to the frequency. The wavelet transformed is given as follows [21]:

$$W(\varsigma,\tau) = \langle f(t), \psi_{\varsigma,\tau}(t)\rangle = \int_{-\infty}^{\infty} f(t)\psi_{\varsigma,\tau}(t)\mathrm{d}t. \tag{3}$$

The inverse transformation [21] into the time domain from the wavelet transformed is defined by

$$f(t) = \frac{1}{C_\psi}\int_0^\infty \int_{-\infty}^{\infty} W(\varsigma,\tau)\frac{1}{\varsigma^2}\psi_{\varsigma,\tau}(t)\,\mathrm{d}\tau\,\mathrm{d}\varsigma. \tag{4}$$

If time signals are discrete, the conditions for applying the DWT are given. For this, a multiscale analysis algorithm is necessary. For 1-D time signals the subband coding by decomposition into coefficients, which serve as a measure of the similarity between the original function and the corresponding basis function with specification of the scaling, is suitable for the implementation [6], [21].

B. DWT: Decomposition Into Coefficients

In general, subband coding is used for analyzing by dividing the signal into individual frequency subbands. Within the DWT, the signal is applied to a low-pass filter and then subsampled (usually by a factor of 2), and applied to a high-pass filter and then subsampled as well. The output of the low-pass filter is again given to such filtering by a new high-pass and low-pass filter. The filter characteristic

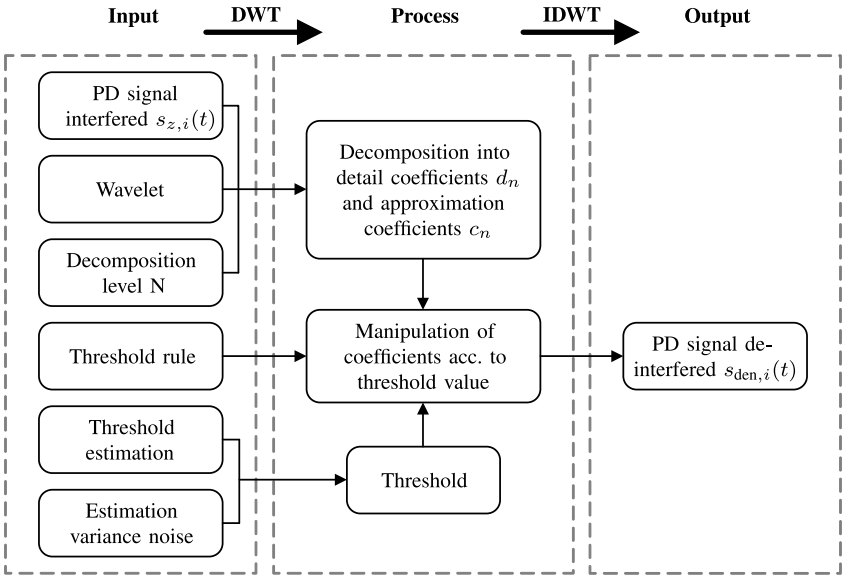

Fig. 9. Principle of wavelet denoising.

is realized by scaling the wavelet. The output values of the lowpasses are called approximation coefficients c_n, those of the highpasses detail coefficients d_n. The procedure is performed N times depending on the level determination. The detailed calculation of the coefficients is provided in [5], [6] and [21].

C. Threshold Rule and Threshold Estimation

During the wavelet denoising procedure, a threshold function $\eta_T(w)$ is applied to the wavelet coefficients. The wavelet coefficients $w = \{c_n, d_n\}$ are adjusted in case of a hard threshold rule [5], [6] according to

$$\eta_T(w) = \begin{cases} w, & \text{for } |w| \geq T \\ 0, & \text{for else} \end{cases} \tag{5}$$

and in case of a soft threshold rule [5], [6] according to

$$\eta_T(w) = \begin{cases} w - T, & \text{for } w \geq T \\ w + T, & \text{for } w \leq -T \\ 0, & \text{for else.} \end{cases} \tag{6}$$

The threshold T is estimated by appropriate procedures using cost functions. A well-known method is the Stein's unbiased risk estimator (SURE), where the estimation of the risk is done with a quadratic loss function [6]. Within the Bayes Estimator (Bayes), the estimation is done by modeling a distribution according to Bayes' theorem. Within the false discovery date estimator (FDR), a good ratio between false matches and as many correct matches as possible is formulated and estimated. The Minimax Estimator attempts to minimize the mean squared error compared to an ideal procedure. The Universal Threshold uses the estimation procedure of the Minimax Estimator and multiplies the threshold by a proportionality factor [7].

The variance of the noise is also unknown and has to be estimated. This is done either level-independent based on the highest level wavelet coefficient or level-dependent based on the wavelet coefficient of each resolution level. More information and further literature are given in [7].

V. Evaluation Process

A. Parameters for Evaluating Interference Suppression

The noise reduction is evaluated by the SNR

$$\mathrm{SNR} = 10 \cdot \log\left(\frac{\sum_{i=1}^{n} s_i(t)^2}{\sum_{i=1}^{n} z_i(t)^2}\right) \tag{7}$$

in dB, which is the ratio between the average useful signal power and the average interference power [5]. A positive value means that the average useful signal power is higher than the average interference power. In noncontact PD measurements by antennas, the mean power of the PD signal is often much lower than the power of the interference environment signals. Therefore, negative dB values are expected here.

To calculate the SNR, a case differentiation is made between the generation of the synthetic PD signal and the evaluation of the process with the synthetic test signal. By generating the disturbed synthetic PD signal, an interference signal $z_i(t)$ measured in the laboratory environment is added to the synthetic PD signal $s_i(t)$ to $s_{z,i}(t) = s_i(t) + z_i(t)$, resulting in the intended SNR before interference suppression. Correspondingly, $s_{\mathrm{den},i}(t)$ describes the signal after interference suppression. After passing through the interference suppression process, the signal $s_{\mathrm{den},i}(t)$ still contains residual interference. The SNR of the signal resulting from the interference suppression process is determined accordingly by relating the ideal artificial PD signal to the remaining interference component $s_{\mathrm{den},i}(t) - s_i(t)$.

Another case distinction is obtained by calculating the SNR using the measured PD signal. Here, the SNR of the measurement signal detected by the antenna is estimated by relating the signal $s_{\mathrm{den},i}(t)$ after interference suppression to the suppressed interference $s_{z,i}(t) - s_{\mathrm{den},i}(t)$. Since no ideal interference-free signal is available as an expected value, the remaining residual noise after the suppression process is impossible to determine.

A further criterion for evaluating interference reduction is the noise reduction rate

$$\mathrm{NRR} = 10 \cdot \log\left(\frac{\sigma_{s,z}^2}{\sigma_{s,\mathrm{den}}^2}\right) \tag{8}$$

in dB [15], [19]. Here, the deviation of the signals before and after interference suppression is related to each other. The higher this value, the more positively the SNR is influenced.

B. Parameters for Evaluating Signal Distortion

To evaluate the influence of the interference suppression process on the usable input signal, the synthetic PD signal $s_i(t)$, which is superimposed with interference to $s_{z,i}(t)$ and passes the interference suppression process, is formulated as an expected value. Based on this expected value, the distortion of the resulting denoised signal $s_{\mathrm{den},i}(t)$ is determined. On the one hand, the MSE

$$\mathrm{RMSE} = \sqrt{\frac{1}{N}\sum_{i=1}^{n}\left(s_{\mathrm{den},i}(t) - s_i(t)\right)^2} \tag{9}$$

[15], [17], [18] and on the other hand the correlation coefficient

$$\mathrm{Corr} = \frac{1}{N-1}\sum_{i=1}^{n}\left(\frac{s_i(t) - \overline{s_i(t)}}{\sigma_s}\right)\left(\frac{s_{\mathrm{den},i}(t) - \overline{s_{\mathrm{den},i}(t)}}{\sigma_{s,\mathrm{den}}}\right) \tag{10}$$

[8], [15], [19] between the expected value $s_i(t)$ and the actual output signal $s_{\mathrm{den},i}(t)$ is calculated. An RMSE of 0 means that the interference suppression process does not manipulate the synthetic PD signal $s_i(t)$. Here, it must be taken into account that interference components remaining in the signal after the interference suppression also influence the RMSE. Accordingly, especially if the average useful signal power is higher or at least not significantly lower than the interference signal power, this indicator provides an evaluation basis for the influence of the interference suppression process on the useful signal. On the other hand, a Corr of 1 means that the output signal fully matches the expected value, whereas a value of 0 corresponds to no matching. Here, residual noise components in the output signal also influence the value of the parameter.

C. New Reliability Score of Pulse Detection

A new evaluation criterion is introduced, by which the reliability of the pulse detection (RSPD) is evaluated quantitatively. The reliability score of pulse detection RSPD is determined by comparison with the comparison signal measured synchronously at the MC and is used to evaluate whether PD pulses are correctly detected from the signal as such or whether interference pulses are incorrectly detected as PD pulses by

$$\mathrm{RSPD} = \frac{\text{counted pulse events}}{\text{expected pulse events}} \cdot 100. \tag{11}$$

The score is given in %. Amplitudes are identified as pulses if they are 30% above the average of the amount of the basic interference level remaining after interference suppression according to

$$A_p > 1.3 \cdot \frac{1}{n}\sum_{i=1}^{n}|z_{\mathrm{den},i}(t)|. \tag{12}$$

With regard the qualification for online monitoring, the running time Δt of the interference suppression process is analyzed.

To evaluate the interference suppression by using a measured signal, only the NRR and the reliability score of pulse detection RSPD are of interest since the original signal is not available and therefore neither serves as an expected value nor allows the determination of the residual interference.

VI. Results and Discussion

A. Prestudy With Synthetic PD Signals

All wavelets listed in Table I as well as thresholding rules and threshold estimation procedures are applied and combined in the studies. In Tables II and III each of the two most suitable orthogonal and biorthogonal wavelets and the corresponding results of the evaluation criteria are shown. By using the orthogonal wavelets of the *Han linear-phase moments* wavelet family han.5.5 and the *Discrete Meyer* family dmey, the best results are achieved in terms of interference reduction (SNR and NRR) and PD pulse detection (RSPD) at lowest distortion (RMSE and Corr) of the useful PD signal. Comparable results are reached using the biorthogonal wavelets of the *BiorSplines* family bior1.5 and the *ReverseBior* family rbio5.5.

The threshold estimation using the Universal Estimator with hard as well as soft threshold rule and the estimation using the Bayes Estimator and the Minimax Estimator with soft threshold rule are the most suitable. All other methods for threshold estimation result in a reliability score of pulse detection RSPD $> 150\%$, which means that 1/3 of the detected pulses are interfering pulses. Above this value an unacceptable interference suppression performance of the method is assumed, because only in the case of a very large SNR the RSPD is less than 150%. Accordingly, these methods are not suitable for PD pulse detection and are not listed in the presentation of results. An RSPD $> 150\%$ also occurs partially by using the methods shown in Tables II and III, especially using the soft threshold rule.

As far as the running time Δt of the methods is mentioned, all methods are suitable for online monitoring, as none of the processes takes longer than 5 s.

B. Application to Measurement Data

Based on the results of the evaluation using the synthetic PD signals, the best combinations are applied to the measurement signal of the antenna shown in Fig. 5. The results are presented in Table IV. The evaluation criteria regarding the distortion of the signal due to the interference suppression process are not used since no ideal signal is available as an expected value. The NRR as well as the running time Δt and the reliability score of pulse detection RSPD are evaluated. The SNR of the measured signal is estimated by comparison with the

TABLE II
EVALUATION CRITERIA OF INTERFERENCE SUPPRESSION WITH THE ORTHOGONAL WAVELETS HAN LINEAR-PHASE MOMENTS AND DISCRETE MEYER WITH SYNTHETIC PD SIGNAL

Denoising method			Before denoising	After denoising				Δt in s	RSPD in %
Wavelet	Estimator	Rule	SNR in dB	SNR in dB	NRR	RMSE	Corr		
han5.5	Universal	hard	−70.550	−4.540	28.118	0.002	0.652	2.387	113.7
	Universal	soft		−3.919	28.434	0.002	0.665	2.358	109.4
	Bayes	soft		−3.737	28.342	0.002	0.682	3.370	>150
	Minimax	soft		−3.929	28.403	0.002	0.666	2.298	117.9
han5.5	Universal	hard	−48.570	17.026	20.780	0.002	0.942	2.426	113.7
	Universal	soft		15.638	21.239	0.002	0.924	2.314	105.2
	Bayes	soft		17.669	21.026	0.002	0.945	3.340	111.1
	Minimax	soft		16.281	21.183	0.002	0.931	2.310	108.5
han5.5	Universal	hard	−24.500	40.854	10.964	0.002	0.994	2.415	111.1
	Universal	soft		37.088	11.198	0.002	0.990	2.445	100.0
	Bayes	soft		41.094	11.065	0.002	0.994	3.369	104.3
	Minimax	soft		38.352	11.161	0.002	0.992	2.294	102.6
dmey	Universal	hard	−70.550	−4.045	27.852	0.002	0.701	1.320	117.9
	Universal	soft		−3.047	28.194	0.002	0.729	1.212	110.3
	Bayes	soft		−3.188	28.133	0.002	0.726	2.359	>150
	Minimax	soft		−3.133	28.163	0.002	0.726	1.188	>150
dmey	Universal	hard	−48.570	17.587	20.730	0.002	0.947	1.297	116.2
	Universal	soft		17.909	20.885	0.002	0.948	1.192	107.7
	Bayes	soft		18.413	20.837	0.002	0.952	2.234	>150
	Minimax	soft		18.067	20.869	0.002	0.949	1.179	112.0
dmey	Universal	hard	−24.500	40.986	10.962	0.002	0.994	1.272	113.7
	Universal	soft		39.942	11.034	0.002	0.993	1.189	102.6
	Bayes	soft		41.820	10.999	0.002	0.995	2.302	106.8
	Minimax	soft		40.536	11.024	0.002	0.994	1.183	106.8

TABLE III
EVALUATION CRITERIA OF INTERFERENCE SUPPRESSION WITH THE BIORTHOGONAL WAVELETS BIORSPLINES AND REVERSEBIOR WITH SYNTHETIC PD SIGNAL

Denoising method			Before denoising	After denoising				Δt in s	RSPD in %
Wavelet	Estimator	Rule	SNR in dB	SNR in dB	NRR	RMSE	Corr		
bior1.5	Universal	hard	−70.550	−5.651	27.729	0.002	0.617	1.796	104.2
	Universal	soft		−6.107	27.906	0.002	0.572	1.733	100.0
	Bayes	soft		−5.223	27.944	0.002	0.625	2.773	>150
	Minimax	soft		−5.846	27.929	0.002	0.587	1.680	>150
bior1.5	Universal	hard	−48.570	11.280	20.280	0.002	0.885	2.062	103.4
	Universal	soft		9.770	20.761	0.003	0.849	1.807	100.0
	Bayes	soft		11.656	20.570	0.002	0.884	2.876	105.1
	Minimax	soft		10.417	20.720	0.003	0.861	1.766	107.7
bior1.5	Universal	hard	−24.500	18.701	10.465	0.006	0.932	1.890	103.4
	Universal	soft		18.413	10.725	0.006	0.926	2.111	100.0
	Bayes	soft		18.860	10.582	0.006	0.931	3.445	108.5
	Minimax	soft		18.609	10.685	0.006	0.928	1.825	100.0
rbio5.5	Universal	hard	−70.550	−4.595	28.061	0.002	0.654	2.430	111.9
	Universal	soft		−4.356	28.367	0.002	0.644	2.398	106.8
	Bayes	soft		−3.828	28.316	0.002	0.678	3.458	>150
	Minimax	soft		−4.244	28.352	0.002	0.652	2.376	120.5
rbio5.5	Universal	hard	−48.570	17.002	20.753	0.002	0.942	2.453	111.9
	Universal	soft		15.016	21.186	0.002	0.918	2.361	105.1
	Bayes	soft		17.496	21.000	0.002	0.944	3.435	>150
	Minimax	soft		15.798	21.140	0.002	0.926	2.376	106.8
rbio5.5	Universal	hard	−15.710	39.606	10.956	0.002	0.993	2.428	110.3
	Universal	soft		35.812	11.178	0.002	0.989	2.354	100.0
	Bayes	soft		39.524	11.054	0.002	0.993	3.405	105.9
	Minimax	soft		37.032	11.144	0.002	0.990	2.332	101.7

interference suppressed signal. Based on the RSPD and NRR, the han5.5 wavelet (RSPD = 103.5%) and the rbio5.5 wavelet (RSPD = 104.6%) using the Universal Estimator with soft threshold rule are proven to be the optimal combination for the interference suppression process to be applied to the noncontact and broadband detected measurement signal.

TABLE IV
EVALUATION CRITERIA OF INTERFERENCE SUPPRESSION USING MEASURED SIGNALS DETECTED BY CONTACTLESS BROADBAND ANTENNA

Denoising method			Consideration	After denoising	Δt in s	RSPD in %
Wavelet	Estimator	Rule	SNR in dB	NRR		
han5.5	Universal	hard	−59.120	25.805	2.330	103.5
	Universal	soft	−63.454	27.750	2.350	101.5
	Bayes	soft	−60.704	26.514	3.454	120.6
	Minimax	soft	−62.918	27.508	2.383	109.9
dmey	Universal	hard	−58.686	25.611	2.429	106.9
	Universal	soft	−63.178	27.625	2.437	103.1
	Bayes	soft	−60.224	26.299	3.516	118.3
	Minimax	soft	−62.582	27.357	2.469	111.5
bior1.5	Universal	hard	−57.900	25.265	1.748	107.6
	Universal	soft	−62.672	27.400	1.751	103.1
	Bayes	soft	−59.600	26.024	2.886	113.0
	Minimax	soft	−62.124	27.154	1.760	117.6
rbio5.5	Universal	hard	−59.010	25.756	2.388	104.6
	Universal	soft	−63.304	27.683	2.380	101.5
	Bayes	soft	−60.578	26.458	3.535	113.0
	Minimax	soft	−62.768	27.441	2.386	111.5

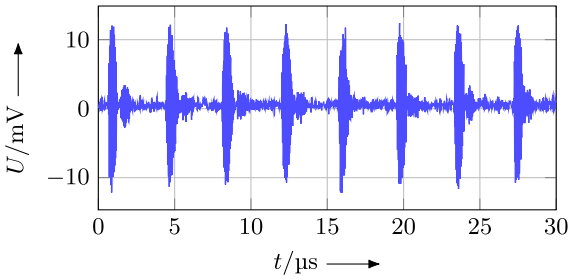

Fig. 10. Interference suppressed measured PD signal with han5.5 and universal threshold hard-section with 8 PD of a signal with over 100 PD.

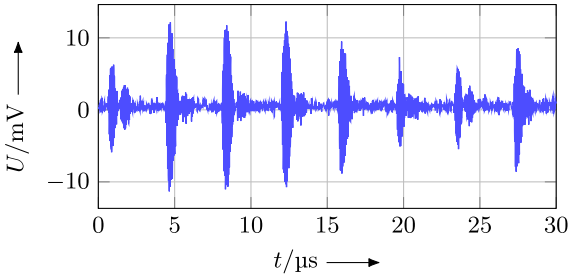

Fig. 11. Interference suppressed measured PD signal with han5.5 and universal threshold soft-section with 8 PD of a signal with over 100 PD.

A closer look at the time signals in Figs. 10 and 11 shows that due to the soft threshold rule the amplitudes of the PD pulses are strongly distorted, according to the scattering of the amplitude of the PD pulses. Compared to the interference-free measurement signal from the measurement cell shown in Fig. 4 and the reference wire signal shown in Fig. 3, there is less expectable scatter in the maximum amplitudes of the PD pulses. This indicates the necessary further formulation of an additional evaluation criterion, which evaluates the influence on the scatter of the amplitudes of the PD pulses, especially with regard to a calibration within the context of the charge determination.

In the evaluation process by using the synthetic signal, this distortion of the pulse amplitudes also appears during the visual review of the interference-suppressed signals. Applying the threshold rule according to (6), all coefficients that are not set to 0 are manipulated by the amount of threshold T, while under the hard threshold rule according to (5) all coefficients that are not set to 0 are kept unchanged. This causes a nonnegligible distortion of the scattering in the amplitudes of the PD pulses. It has to be taken into account that by using the soft threshold rule in combination with other estimation methods at least a better pulse detection is realized than with the hard threshold rule.

VII. CONCLUSION AND OUTLOOK

Within the preliminary investigations with synthetic interfered PD signals concerning the combination of all wavelets, threshold estimation methods and threshold rules listed in Table I, the orthogonal wavelets han5.5 and dmey as well as the biorthogonal wavelets bior1.5 and rbio5.5 prove to be the most qualified. By using the Universal Estimator with hard and soft threshold rule as well as the Bayes Estimator and the Minimax Estimator each using the soft threshold rule, best pulse detection, and reconstruction is possible. From the study with a synthetic signal, it is shown that these combinations isolate all PD pulses and only a few interfering pulses even in case of a strong noise and interference superposition of the input signal.

Applying the most suitable wavelets and threshold estimators to the PD measurement signals as shown in Table IV, the best results are obtained using the han5.5 wavelet or the bior1.5 wavelet with Universal Estimator and hard threshold rule. The reliability score of pulse detection RSPD proves to be the most important quality criterion.

A more detailed view at the interference-suppressed signals shows that the amplitudes of the PD pulses are distorted by the soft threshold rule, which leads to problems in the charge determination. This results in the requirement of formulating a further evaluation criterion, whereby the influence and distortion of the amplitudes in the signal are evaluated and, if necessary, corrected by a correction factor dependent on the interference suppression method, in particular with regard to a calibration procedure in the context of a charge determination.

With regard to the evaluation criteria, it is clear that criteria evaluating the influence of the interference suppression process

on the useful signal (RMSE and Corr) and the interference reduction (SNR and NRR) are of importance. Furthermore, it becomes evident that a new formulated criterion for the RSPD provides a considerable contribution to the evaluation of interference suppression methods in the context of PD diagnosis. Through the use of this new criterion, it becomes quantifiable if the PD pulses are isolated from the signal by the interference suppression process and useful for further processing such as classification or charge determination. Regarding the running time, all methods have a running time of less than 5 s and are therefore suitable for online monitoring.

REFERENCES

[1] *Hochspannungs-Prüftechnik: Teilentladungsmessungen*, Standard DIN EN 60270, VDE 0434, 2016.

[2] A. J. Schwab and W. Kürner, *Elektromagnetische Verträglichkeit (VDI-Buch)*. Berlin, Heidelberg: Springer, 2011, doi: 10.1007/978-3-642-16610-5.

[3] G. König, "Ein adaptives digitales Filterverfahren zur Unterdrückung hochfrequenter periodischer Störungen bei Teilentladungsmessungen," Ph.D. dissertation, Fakultät Elektrotechnik der Universität Stuttgart, Institut für Energieübertragung und Hochspannungstechnik, Stuttgart, Germany, 1991.

[4] U. Köpf, "Kontinuierliche Unterdrückung von schmalbandigen, periodischen und breitbandigen, impulsformigen Störern bei der Teilentladungsmessung," Ph.D. dissertation, Fakultät Elektrotechnik der Universität Stuttgart, Institut für Energieübertragung und Hochspannungstechnik, Germany, 1994.

[5] A. Mertins, *Signaltheorie: Grundlagen der Signalbeschreibung, Filterbänke, Wavelets, Zeit-Frequenz-Analyse, Parameter- und Signalschätzung*. Cham, Switzerland: Springer, 2020.

[6] Bergh, F. Ekstedt, and M. Lindberg, *Martin: Wavelets mit Anwendungen in Signal- und Bildverarbeitung*. Cham, Switzerland: Springer, 2007.

[7] Help Center. *MathWorks*. Accessed: Aug. 1, 2023. [Online]. Available: https://de.mathworks.com/help/wavelet/ref/wdenoise.html

[8] D. Evagorou, A. Kyprianou, P. L. Lewin, A. Stavrou, V. Efthymiou, and G. E. Georghiou, "Evaluation of partial discharge denoising using the wavelet packets transform as a preprocessing step for classification," in *Proc. Annu. Rep. Conf. Electr. Insul. Dielectric Phenomena*, Quebec, QC, Canada, Oct. 2008, pp. 387–390, doi: 10.1109/ceidp.2008.4772794.

[9] S. Madhupriya, R. V. Maheswari, and B. Vigneshwaran, "Measurement and denoising of partial discharge signal in high voltage cables using wavelet transform," *Int. J. Eng. Adv. Technol.*, vol. 9, no. 2, pp. 2461–2468, Dec. 2019, doi: 10.35940/ijeat.b3991.129219.

[10] V. H. A. Vidya, H. A. B. Tyagi, V. K. V. Krishnan, and K. M. K. Mallikarjunappa, "Removal of interferences from partial discharge pulses using wavelet transform," *TELKOMNIKA Telecommun. Comput. Electron. Control*, vol. 9, no. 1, p. 107, Apr. 2011, doi: 10.12928/telkomnika.v9i1.675.

[11] A. Zaeni, T. Kasnalestari, and U. Khayam, "Application of wavelet transformation symlet type and coiflet type for partial discharge signals denoising," in *Proc. 5th Int. Conf. Electric Veh. Technol. (ICEVT)*, Surakarta, Indonesia, Oct. 2018, pp. 78–82, doi: 10.1109/ICEVT.2018.8628460.

[12] A. Zaeni, T. Kasnalestari, and U. Khayam, "Partial discharge signal denoising by using hard threshold and soft threshold methods and wavelet transformation," in *Proc. IOP Conf. Ser., Mater. Sci. Eng.*, 2019, pp. 1–8, doi: 10.1088/1757-899X/602/1/012034.

[13] Ö. Altay and Ö. Kalenderli, "Wavelet base selection for de-noising and extraction of partial discharge pulses in noisy environment," *IET Sci., Meas. Technol.*, vol. 9, no. 3, pp. 276–284, May 2015, doi: 10.1049/iet-smt.2013.0114.

[14] J. Li, T. Jiang, S. Grzybowski, and C. Cheng, "Scale dependent wavelet selection for de-noising of partial discharge detection," *IEEE Trans. Dielectr. Electr. Insul.*, vol. 17, no. 6, pp. 1705–1714, Dec. 2010, doi: 10.1109/TDEI.2010.5658220.

[15] X.-C. Hua et al., "A novel adaptive parameter optimization method for denoising partial discharge ultrasonic signals," *IEEE Trans. Dielectr. Electr. Insul.*, vol. 30, no. 6, pp. 2734–2743, Dec. 2023, doi: 10.1109/tdei.2023.3331663.

[16] Q. Lin, F. Lyu, S. Yu, H. Xiao, and X. Li, "Optimized denoising method for weak acoustic emission signal in partial discharge detection," *IEEE Trans. Dielectr. Electr. Insul.*, vol. 29, no. 4, pp. 1409–1416, Aug. 2022, doi: 10.1109/TDEI.2022.3183662.

[17] R. Hussein, K. B. Shaban, and A. H. El-Hag, "Energy conservation-based thresholding for effective wavelet denoising of partial discharge signals," *IET Sci., Meas. Technol.*, vol. 10, no. 7, pp. 813–822, Oct. 2016, doi: 10.1049/iet-smt.2016.0168.

[18] M. I. Sharif, J. P. Li, and A. Sharif, "A noise reduction based wavelet denoising system for partial discharge signal," *Wireless Pers. Commun.*, vol. 108, no. 3, pp. 1329–1343, Oct. 2019, doi: 10.1007/s11277-019-06471-2.

[19] C. Boya-Lara, O. Rivera-Caballero, and J. A. Ardila-Rey, "A comparative study of denoising techniques for UHF signals from partial discharge," in *Proc. 8th Int. Eng., Sci. Technol. Conf. (IESTEC)*, Panama, Oct. 2022, pp. 595–601, doi: 10.1109/IESTEC54539.2022.00099.

[20] S. Lan, Y.-Q. Hu, and C.-C. Kuo, "Partial discharge location of power cables based on an improved phase difference method," *IEEE Trans. Dielectr. Electr. Insul.*, vol. 26, no. 5, pp. 1612–1619, Oct. 2019, doi: 10.1109/TDEI.2019.008202.

[21] O. Hochmuth and B. Meffert, *Werkzeuge der Signalverarbeitung: Grundlagen, Anwendungsbeispiele, Übungen*. Berlin, Germany: Humboldt Univ. Berlin, 2018.